# A Film Print Spectrum Recovery Method for LED and Laser-Based Digital Cinema Display Systems

Michael T. Lauter
*MindCine*, PO Box 181696, Denver, CO 80218 USA – mindcine.com
14 September 2008

## ABSTRACT

Lasers, LEDs and other nearly monochromatic photonic devices offer great potential for realizing full-gamut color reproduction in digital cinema display system. The downside of such spectrally narrow light sources is that – for any given tristimulus color coded input – there is greater variations in color perception among viewers, as compared to conventional Xenon light sources. This paper describes a laser-based cinema display design and its associated real-time processing techniques for 4K resolution film print spectrum estimation. The recovered spectrum metaristicaly matches its DCI's *X'Y'Z'* color coding input signal, simultaneously accounting for the Mespoic and Scotopic human visual response at very lower light levels.

**Keywords**: spectrum recovery, spectrum estimation, spectral imaging, colorimetry, color semitometry, metarism, DCI (Digital Cinema Initiative), Mesopic vision, Scotopic vision, high dynamic range (HDR), laser image display, 4K cinema, Cell Broadband Engine, CUDA.

## INTRODUCTION

Nearly monochromatic light sources such as lasers and light-emitting diodes lend themselves well to full-gamut color reproduction. However, using such light sources produce in tristimulus display systems causes greater variations in color perception among viewers, as compared to full spectrum (Xenon) projection lamps. Despite this drawback, the benefits of laser-based displays are many. For instance, they are free of lens flare associated with current projection technologies – either film or DLP. The virtual elimination of flare greatly increases contrast and achievable dynamic range. With purely emissive LED and Laser displays, reflective white screens are not required, so the achievable black levels will be much, much lower. For some scene content, the Scotopic range of human vision must be addressed. This paper introduces a method of synthetically recovering film print spectra that materistically matches the (Digital Cinema Initiative's) DCI's *X'Y'Z'* color coding, while simultaneously accounting for the Scotopic Human visual response at very lower light levels. The application of these display technologies combined with spectral estimation should greatly benefit critical color film grading suites as well as theaters. While the technique described herein could be considered a 'film-centric' DCI mastering workflow, is still offers benefits to 'digital-centric' mastering as well. The method also adapts well to other color-critical applications in traditional printing, medicine, architectureal design and aerospace.

## DESIGN CONSIDERATIONS

There are two conceptual approaches to using lasers for cinema. The first having steered light beams projected onto a typical reflective white or silver screen. Another design would have a large grid of multiple, lower-powered lasers - one for every display pixel - creating an emissive screen, not altogether different in concept to laser TVs. Both concepts eliminate the ubiquitous cinema projection lens and its associated flare, keystoning and potential focus problems. The emissive design case further eliminates the need for a reflective screen. In fact, the screen surface might have anti-reflective coating with localized diffusion and de-speckling characteristics. In this case, a greater dynamic range would be achievable. The dark areas of the screen would have deeper blacks than currently found in the cinema – with even the best low-flare optics and densest prints stocks (Kodak Vision2 Premier 2393). For very dark scenes, as found in thrillers and horror films, the discernible dark hues irradiate below the Photopic range; into the Mesopic and further into below into the Scotopic ranges of human vision, [Ref. 9] where the eye relies upon the retina's rods in addition to its cones.

### Industry trends

Current cinema mastering in the motion picture industry is predominately in being done with Digital Intermediate (DI) or other high-definition digital tools. The Cineon / DPX log density colorspace was once a master format, deeply rooted in a photochemical model. Now the trend is to master first in full-gamut DCI *X'Y'Z'* colorspace and force and film prints to best match, even if gamut mapping is required. The laser display must be able to be faithful to both DCI-centric and the Photochemical-centric masters.

## SYSTEM DESIGN

Currently, single-mode lasers are available with wavelengths in the 400 nm to 700 nm visual spectrum. The proposed system would have a pool of sixteen (16) available laser wavelengths at roughly 20 nm intervals. From this pool eight (8) could emit simultaneously. It is not necessary for the sources to have exact spectrum spacing. As long as they are not too clustered, the system will work. Because of physical limitations, it may not be possible to have all sixteen source emit at once, so eight are chosen for each pixel, again roughly spaced, i.e., approximately 40 nm apart. We call the nomochromatic sources Virutal Emissive (VEs). The emissive display could alternate pixel by adjacent pixel.

| | wavelength in nm | | | | | | | | | | | | | | | |
|---|---|---|---|---|---|---|---|---|---|---|---|---|---|---|---|---|
| “ideal” | 400 | 420 | 440 | 460 | 480 | 500 | 520 | 540 | 560 | 580 | 600 | 620 | 640 | 660 | 680 | 700 |
| realizable | 403 | 419 | 445 | 467 | 482 | 496 | 517 | 539 | 555 | 579 | 606 | 618 | 635 | 663 | 670 | 697 |
| name | VE1 | VE2 | VE3 | VE4 | VE5 | VE6 | VE7 | VE8 | VE9 | VE10 | VE11 | VE12 | VE13 | VE14 | VE15 | VE16 |

Odd-numbered VEs then even-numbered; alternating between [$VE_1$ $VE_3 \ldots$ $VE_{15}$] and [$VE_2$ $VE_4 \ldots$ $VE_{16}$]. This spectro-spatial decimation is perfectly valid for 4K images since human vision has less acutance in chromaticity than in luminance. [Ref. 11] Of course, if displays are able of simultaneously emitting sixteen sources per pixel, then the technique herein described can accommodate.

## MATHEMATICAL METHODS

The processing described here details the per-pixel computations. Naturally, the input is the DCI-compliant color coding of *X'Y'Z'* tristimulus values. The prime notation (') indicates that a gamma is applied to the CIE (Commission internationale de l'éclairage) *XYZ* color matching values.

### Film Print Dye synthesis

The *X'Y'Z'* input is translated into print dye concentration values *CMYK*; Cyan, Magenta, Yellow, and Black. ***Why Black?*** Color transparencies do not have black dye! The reasoning for including black is that it opens up exciting possibilities for reproducing fine art in the cinema. If we are going through the trouble of modeling the photographic dyes, why not include spectrally neutral ones in our palette? There are great creative possibilities for modeling "Theoretical Photographic Dyes" with well-behaved spectral qualities. For emulating existing, real-life print film stocks and their dyes, the Black dye concentration is simply set to zero, *K*=0.

Note that *CMY* dye concentrations should not be confused with ISO Status-A densities; $D_B$, $D_G$, $D_R$. It is possible, however, to transform Status-A densities into *CMY* values or the inverse via matrix math. [Ref. 3] Further note that, the three Status-A densities are covariant, or dependent upon each other, while dyes concentrations are independent. For modeling spectral characteristics and color analysis of film prints, *CMY* values or much more useful.

### Look-up-tables (LUTs)

The translation from *X'Y'Z'* values to *CMY[K]* values requires some knowledge about the spectral qualities of the dyes and the viewing (reference) illuminant; a typical Xenon lamp. As will be shown later, the CIE Scotopic Luminance Efficiency *V** must be also be derived. So we first create a *CMY* → *X'Y'Z'V'* 3D Look-Up-Table (LUT). Then this LUT in partially inverted by interpolation to create a new LUT such that *X'Y'Z'* → 3DLUT → *CMY[K]V'* where *K*=0. Note that in the future if *V'* values are encoded per pixel, then there are enough values to recover singular Black dyes, *K* values with 4D (four-dimensional LUTs), for example *X'Y'Z'V'* → 4DLUT → *CMYK*.

For *X'Y'Z'* inputs which correspond to an out-of-film-gamut color, the system can revert to the idealized dyes (wider) gamut or further to a "spectral locus proximity mode" full gamut color model.

### Dye Modeling

Once CMY[K] concentration values are derived, they are then used to synthesize the film print's integral spectral density, *D(λ)*. This model is used twice; for the initial 3D LUT creation (one-time) and for the per-pixel (real-time) spectral power distribution. For the one-time LUT generation, the integral spectral density in synthesized from 390 – 705 nm at 5 nm resolution. The continuous-spectrum version of the equation is:

$$D(\lambda) = C\ D_C(\lambda) + M\ D_M(\lambda) + Y\ D_Y(\lambda) + K\ D_K(\lambda) + D_{min}(\lambda)$$

$Dc(\lambda)$, $Dm(\lambda)$, $Dy(\lambda)$ and $Dk(\lambda)$ are the characteristic spectral density curves for the dyes. $D_{min}(\lambda)$ is spline-interpolated from ISO Status-A density measurements for $D_{min}$, or the print base density, typically [0.07, 0.07, 0.10], corresponding (roughly and) respectively to 620 nm, 530 nm and 440 nm. [Ref. 2] The $C$, $M$ , $Y$ , and (optionally) $K$ are the dyes concentration values. The scaling of these characteristic dye density curves by their associated concentration values assumes that the dyes obey Beer's Law. In practice this model does not precisely match the dye-depositing characteristics of real film prints. However, the dyes in film emulsions follow Beer's law reasonably well [Ref. 12] and the model is sufficient for creating a two-way metarisitic link between $XYZ(V)$ and spectral colorimetry.

Illustration **I** shows the various dye deposit curves (colored lines) and their integral spectral density (black line). The dashed line is the interpolated base spectral density derived from $D_{min}$. The Black dye concentration, $K$, is set to zero.

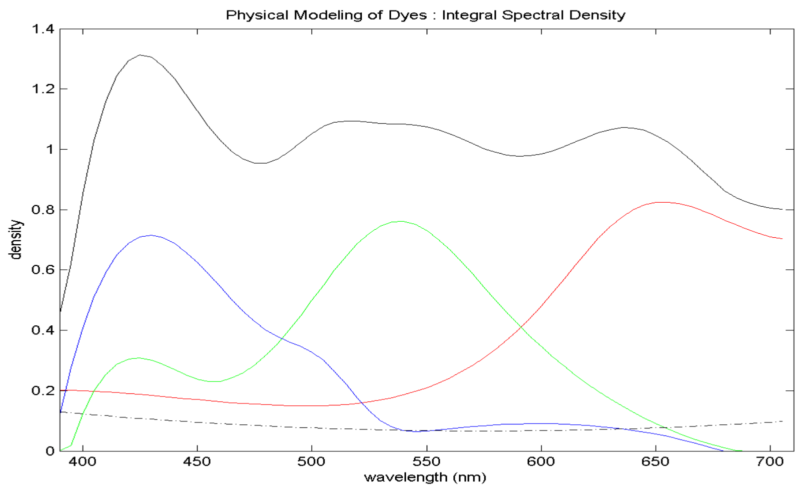


*Illustration I: Integral Spectral Density*

The nominal dye deposit curves are scaled such that for concentration values of unity, $C=M=Y=1$, the resulting integral is an "equivalent neutral density" of one. Because it is not perfectly neutral across the spectrum, the underlying assumption is that for a given reference illuminant, the integral *appears* neutral. The choice of **D65** *vs.* **D55** *vs.* **DCI Ref. Proj.**, or even a blackbody locus illuminant requires slight scaling of the $D_C(\lambda)$ $D_M(\lambda)$ $D_Y(\lambda)$ curves to create neutral density for $C+M+Y=1$. This aids the argument for the inclusion of (virtual) black dyes which are indeed spectrally neutral, giving perfect gray-scale reproduction for fine art and B&W images, regardless of illuminant choice.

An alternative is to use "idealized dyes," which have perfectly orthogonal relationships and possess the quality of achieving perfect spectral neutrality. The dashed lines in Illustration **II** show idealized dyes compared to real-life dyes.

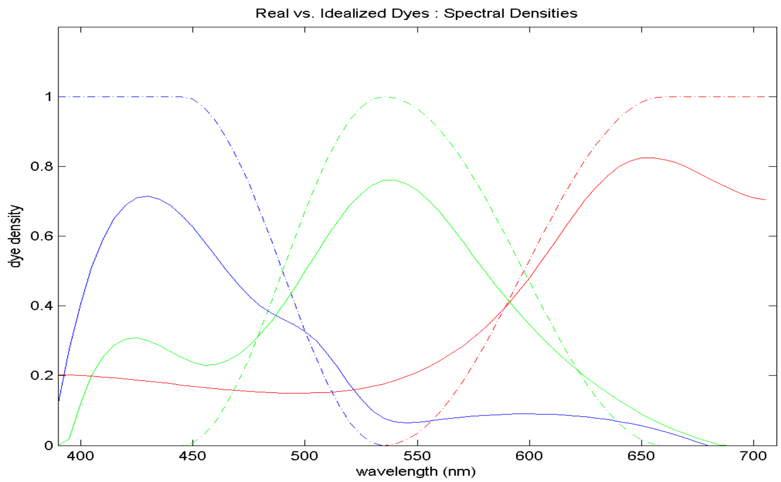

*Illustration II: Real vs. Ideal Transparency Dyes*

The discreet sample version of the integral spectral density equation is:

$$D_\lambda = C\,Dc_\lambda + M\,Dm_\lambda + Y\,Dy_\lambda + K\,Dk_\lambda + Dmin_\lambda \qquad K=0$$

With 5 nm resolution sampling from 390 nm to 705 nm, this creates 64 spectral density 'bins.'

The *XYZV* values are computed with well-known equations [Ref. 19] for transmissive and/or reflective materials, discreet case:

$$X=\frac{1}{N}\sum_\lambda \bar{x}_\lambda S_\lambda I_\lambda \quad Y=\frac{1}{N}\sum_\lambda \bar{y}_\lambda S_\lambda I_\lambda \quad Z=\frac{1}{N}\sum_\lambda \bar{z}_\lambda S_\lambda I_\lambda \quad V=\frac{1}{N}\sum_\lambda \bar{v}_\lambda S_\lambda I_\lambda$$
$$N=\sum_\lambda \bar{y}_\lambda S_\lambda I_\lambda$$

Where $S_\lambda$ is the spline-interpolated integral spectral print density and $I_\lambda$ is the reference illuminant's spectral irradiation.

It is worth noting that the Scotopic Luminance Efficiency function *V(λ)* helps represent the 500 nm region of the visible electromagnetic spectrum, which is otherwise not well represented by the other functions, *X Y* and *Z*. This is an important function for properly 'shaping' the recovered spectra.

Next we recall that density of the print is the a logarithm of flux transmittance, $\tau$. (Note: all logarithms herein are base ten.)

$$D_\tau = -\log(\tau) \quad \text{or} \quad D_\tau(\lambda) = -\log(\tau(\lambda))$$

$$D_\lambda = -\log(\tau_\lambda)$$

What we really want is the radiant flux, $\Phi(\lambda)$, or alternate notation, $P(\lambda)$. [Ref. 1] Since the illuminant can be expressed in logarithmic power and densities are also logarithmic, it is possible to subtract density from log flux.

$$\log(\Phi_\lambda) = \log(I_\lambda) + \log(A_\lambda) + \log(\tau_\lambda)$$

$$\log(\Phi_\lambda) = \log(I_\lambda) + \log(A_\lambda) - D_\lambda$$

Note that $A(\lambda)$ is the combined spectral lens transmission and spectral screen reflection; is logarithm is the *apparent spectral density* of the projection setting. This model is used loosely for adjustment of projection environments, sans illuminant. It is not a rigorous physical model. Lens flare modeling needs additional mathematics and while *it is absolutely required* for critical photochemical film grading [Ref. 3], we have ignored it here to focus on the digital cinema exhibition mode with its greater image dynamic range and contrast. Exclusion of the lens flare dynamics – again - does not prevent a *X'Y'Z'* metarism-matching output spectrum.

The flux modeling equations can be replaced into the CIE functions to obtain the following form:

$$Y = \frac{1}{N}\sum_\lambda \bar{y}_\lambda 10^{(\log(\Phi_\lambda))} = \frac{1}{N}\sum_\lambda \bar{y}_\lambda 10^{(\log(I_\lambda) + \log(A_\lambda) - D_\lambda)}$$

$$N = \sum_\lambda \bar{y}_\lambda 10^{(\log(I_\lambda) + \log(A_\lambda))}$$

$$Y' = Y^{\left(\frac{1}{2.6}\right)}$$

$$CV_{Y'} = \mathrm{INT}\left[4095 \cdot \left(\frac{Y}{52.37}\right)^{\frac{1}{2.6}}\right] = \mathrm{INT}\left[\,893.446 \cdot Y'\,\right]$$

From this these equations, the 3D LUT for *CMY* → *X'Y'Z'V'* and its inverted LUTs *X'Y'Z'* → *CMY* and *X'Y'Z'* → *V'* can be computed. Alternatively, *V* can be algebraically derived, as a function of *X*, *Y* and *Z*. In future, *XYZV* encoding can allow for 4D LUTs *X'Y'Z'V'* → *CMYK*. Note that the DCI 12-bit integer coding values, CV, should be used the LUTs, to minimize computation. [Ref. 17] Note further that the equations in this article use normalized *Y* values [0.0 to 1.0] where $Y=1$ is "open gate" projector condition. DCI *Y* value are absolute cd/m² metrics, so the scaling factor 52.37 must be accounted for.

## First Iteration

For the real-time, per-pixel spectrum estimation, we synthesize decimated spectra. The first iteration looks only at the integral spectral densities at the wavelength associated with the virtual emissive sources (VEs). Since the system is designed to encode the VE's wavelength at a much higher 0.125 nm resolution, the *xyzv* color matching coefficients are spline-interpolated once during initialization and stored in local registers. For each VE, the corresponding spectral density, $D(\lambda_{VEn})$, reference spectral illuminance, $I(\lambda_{VEn})$ and subsequent spectral irradiation $\Phi(\lambda_{VEn})$ are computed in real-time. This will be either eight or sixteen spectral lines of radiance per pixel, depending on the system configuration. These density and illuminant samples can be linearly interpolated or simply copied from the nearest 5 nm-resolution samples. Computational errors and approximations here do not prevent an exact metaristic color match. These spectral power lines are first iterations of the spectrum recovery.

**Spectral refinement via metarism**
Now the really interesting matrix mathematics and the core of the algorithm are revealed. Once the first iteration of the decimated spectral radiance is computed, the second and final computation conforms the recovered spectra to exact *XYZV* color matching.

$$\boldsymbol{M} = \boldsymbol{T}\ \boldsymbol{P}$$

$$\begin{bmatrix} X \\ Y \\ Z \\ V \end{bmatrix} = \begin{bmatrix} \bar{x}_1 & \bar{x}_2 & \bar{x}_3 & \bar{x}_4 & \bar{x}_5 & \bar{x}_6 & \bar{x}_7 & \bar{x}_8 \\ \bar{y}_1 & \bar{y}_2 & \bar{y}_3 & \bar{y}_4 & \bar{y}_5 & \bar{y}_6 & \bar{y}_7 & \bar{y}_8 \\ \bar{z}_1 & \bar{z}_2 & \bar{z}_3 & \bar{z}_4 & \bar{z}_5 & \bar{z}_6 & \bar{z}_7 & \bar{z}_8 \\ \bar{v}_1 & \bar{v}_2 & \bar{v}_3 & \bar{v}_4 & \bar{v}_5 & \bar{v}_6 & \bar{v}_7 & \bar{v}_8 \end{bmatrix} \times \begin{bmatrix} P_1 \\ P_2 \\ P_3 \\ P_4 \\ P_5 \\ P_6 \\ P_7 \\ P_8 \end{bmatrix}$$

We want to work with square matrices and we must include a term for the error from the first iteration. The equation can be re-written:

$$\boldsymbol{M} = \boldsymbol{T}_A\ \boldsymbol{P}_A + \boldsymbol{T}_B\ \boldsymbol{P}_B + \boldsymbol{E}_B$$

$$\begin{bmatrix} X \\ Y \\ Z \\ V \end{bmatrix} = \begin{bmatrix} \bar{x}_1 & \bar{x}_3 & \bar{x}_5 & \bar{x}_7 \\ \bar{y}_1 & \bar{y}_3 & \bar{y}_5 & \bar{y}_7 \\ \bar{z}_1 & \bar{z}_3 & \bar{z}_5 & \bar{z}_7 \\ \bar{v}_1 & \bar{v}_3 & \bar{v}_5 & \bar{v}_7 \end{bmatrix} \times \begin{bmatrix} P_1 \\ P_3 \\ P_5 \\ P_7 \end{bmatrix} + \begin{bmatrix} \bar{x}_2 & \bar{x}_4 & \bar{x}_6 & \bar{x}_8 \\ \bar{y}_2 & \bar{y}_4 & \bar{y}_6 & \bar{y}_8 \\ \bar{z}_2 & \bar{z}_4 & \bar{z}_6 & \bar{z}_8 \\ \bar{v}_2 & \bar{v}_4 & \bar{v}_6 & \bar{v}_8 \end{bmatrix} \times \begin{bmatrix} P_2 \\ P_4 \\ P_6 \\ P_8 \end{bmatrix} + \begin{bmatrix} E_2 \\ E_4 \\ E_6 \\ E_8 \end{bmatrix}$$

Where $\boldsymbol{E}_B$ is *XYZV* error, which we assume is contributed by only four of the spectral power lines. We assume the other four are correct.

$$let\ \ \boldsymbol{E}_B = \boldsymbol{T}_B\ \boldsymbol{P}_E$$

$$\boldsymbol{M} = \boldsymbol{T}_A\ \boldsymbol{P}_A + \boldsymbol{T}_B\ \boldsymbol{P}_B + \boldsymbol{T}_B\ \boldsymbol{E}_B$$

$$= \boldsymbol{T}_A\ \boldsymbol{P}_A + \boldsymbol{T}_B\left(\boldsymbol{P}_B + \boldsymbol{P}_E\right)$$

Solve for $\boldsymbol{P}_E$ :

$$\boldsymbol{P}_E = \boldsymbol{T}_B^{-1}\,(\boldsymbol{M} - \boldsymbol{T}_A\,\boldsymbol{P}_A) - \boldsymbol{P}_B$$

$$\text{where } \boldsymbol{T}_B^{-1} = inv(\boldsymbol{T}_B)$$

Another way of thinking of this is that $\boldsymbol{P}_E + \boldsymbol{P}_B$ are the new, replacement values $\boldsymbol{P}_B'$ for the four spectral lines.

$$\boldsymbol{P}_B' = \boldsymbol{P}_B + \boldsymbol{P}_E = \boldsymbol{T}_B^{-1}\,(\boldsymbol{M} - \boldsymbol{T}_A\,\boldsymbol{P}_A)$$

The matrix elements' subscripts suggest the two parts of the matching function are separated by every other spectral line. However, the choice of which four lines to force and which to allow adjustment is determined by the algorithm depending on the color's spectral 'weight.' Improper choice of the fixed lines result in a poorly inverted matrix, $\boldsymbol{T}^{-1}_B$, producing negative power values.

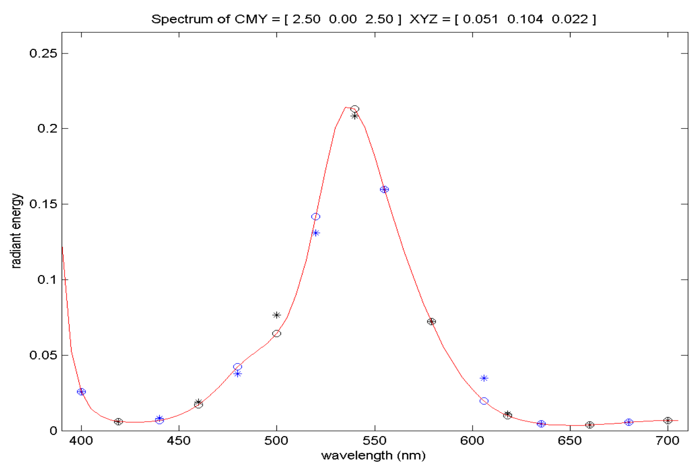


*Illustration III: Example Green Spectrum with Sixteen Emissive Sources*

## RESULTS

Illustrations **III** and **IV** show first iteration spectral targets as circles and the refined spectral power with stars. Note that the values have been scaled for graphing comparisons against the continuous spectral curves. Note further that $Y=1$ is the film projector running “open gate” in the model.

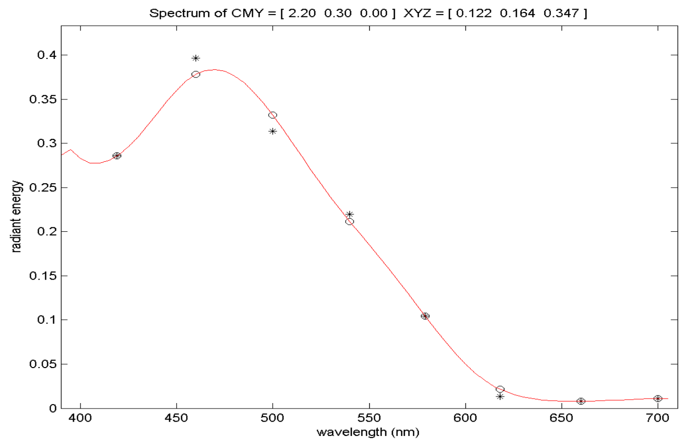


*Illustration IV: Example Cyan Spectrum with eight Emissive Sources*

## REAL-TIME COMPUTATION

The Sony/Toshiba/IBM Cell Broadband Engine and NVIDIA's CUDA parallel computing architecture are both perfectly suited for processing this spectral recovery method in real-time. Let's examine the case of one Cell BE clocked at 3.2 GHz. The processor is theoretically capable of 230 GFLOPs, although best case optimizations with vectorized instructions and double-buffering, can achieve about 180 GFLOPs. **[Ref. 16]** For real-time processing of 4K (4096 x 2160) images at 24 fps (frames per second), **[Ref. 5]** about 213 million pixels must be processed per second. Accounting for overhead, this means there are approximately 900 single-precision (32-bit) floating-point operations available per pixel, per frame.

We must verify that the one Cell BE can handle both data bandwidth and computational bandwidth. From the data bandwidth table below, the worst case data-wise is DSM IN and 16 VEs OUT. Both IN and OUT are far less than a single memory channel's 12.8 GB/sec maximum. **[Ref. 8]**

| 4K Data Stream Type | Pixel Depth & Coding | Data Bandwidth |
|---|---|---|
| Cineon / DPX | 10-bit log printing density | 850 MB/sec |
| DCI “DSM” aka TIFF | 16-bit (12-bit used) X'Y'Z' | 1280 MB/sec |
| DCI “DCP” image only | 12-bit JPEG 2000 | 32 MB/sec |
| DCI “DCP” total | (mixed) | 39 MB/sec |
| Cell BE raw memory I/O | (user-defined) | 12.8 x 2 = 25.6 GB/sec |
| Cell BE EIB (elemental interconnect bus) | (user-defined) | 204 GB/sec |
| Eight VEs | 16-bit | 142 MB/sec |
| Sixteen VEs | 16-bit | 284 MB/sec |

The worst case for computational bandwidth is the DCP (Digital Cinema Package) IN and Sixteen VEs OUT. The JPEG-2000 decoding combined with the spectral recovery processing would require more than one Cell BE for 4K. However, the spectral dye modeling alone requires only one Cell BE. The Cineon/DPX image format is used for the mode of logarithmic color grading of scanned motion picture negatives. [Ref. 4, 7, 14, 15, 18]

The first iteration *CMY[K]* modeling requires very little bandwidth. The refinement via matrix operations take more. A 4x4 matrix multiply requires sixteen Multiply-Accumulate instructions. Each VE requires two 4x4 matrix multiplies. In systems configured with eight VEs, four get matrix-refined, so that's 16x2x4 or 128 Multiply-Accumulate instructions; about 14% of the available bandwidth.

The inversion of a 4x4 matrix $\boldsymbol{T_B}$ to $\boldsymbol{T^{-1}_B}$, is very computationally expensive. [Ref. 10]

$$inv(\boldsymbol{T}_{\boldsymbol{B}}) = \frac{1}{det(\ \boldsymbol{T}_{\boldsymbol{B}}\ )} \cdot adj(\ \boldsymbol{T}_{\boldsymbol{B}}\ )$$

The determinant for a 4x4 matrix and its floating-point reciprocal is the most computationally expensive part of the entire method. However, with the Cell BE's Single Instruction Multiple Data or SIMD vectorization, combined with Vector Permutation and Formatting Instructions and other instruction pipelining, the matrix inversion is possible in single-precision floating point vectors when computing eight (8) VEs values. Sixteen (16) VEs would require two Cell Broadband Engines.

Alternatively, and preferably, since for each eight-VE set there are - according to the binomial "8 choose 4" - 70 possible $\boldsymbol{T^{-1}_B}$ matrices.

$$\binom{8}{4} = \frac{8!}{4! \cdot 4!} = 70$$

If both VE sets (sixteen VEs) are used then that's 140 possible matrices. These can be implemented in an inverted matrix look-up table created at initialization time. With the matrix LUT for $\boldsymbol{T^{-1}_B}$, and using 16 VEs, about 40% of the Cell Broadband Engine's computational bandwidth is used, allowing the remaining 60% for lens flare modeling (in the film grading scenario) or JPEG-2000 decoding. Both VEs sets, 'even' and 'odd,' can be calculated independent of the other and both produce the same *XYZV* values. With both sets used, their $P_{VE}$ spectral power values are simply divided by two.

Further CELL/BE optimization can be achieved by thread parallelism; assigning all operations for a given pixel to a Cell's Synergistic Processor Element (SPE).

## CONCLUSION

In essence, this film spectrum recovery method in a hybrid. While the recovered spectra may not be identical to those of actual projected film prints, they do create a metaristic match to the DCI-coded *X'Y'Z'* colors. From viewer to viewer, the 8 or 16 wavelength laser-based spectrum will more consistently reproduce color compared to other tristimulous color displays.

## ACKNOWLEDGEMENTS

The author wishes to acknowledge the generosity of Wyndham Hannaway of GW Hannaway & Associates, Ray Feeney of RFX, Inc. and Jeff Grazi of Grazi Communications for their input on early drafts of this article.

## RESEARCH REFERENCES

1. ANSI
American National Standard for Photography (Sensitometry) -
Density Measurements – Terms, Symbols, and Notations

2. ANSI PH2.16 84
Density Measurements – Part 3: Spectral Conditions
ANSI/ISO 5-3-1995

3. Brendel, Harald
*The ARRI Companion to Digital Intermediate*, Second Edition
Arnold & Richter Cine Technik GmbH and Co. (ARRI, Inc.)
September 2005

4. Case, Dominic
*Film Technology in Post Production*, Second Edition
Focal Press 2001

5. Digital Cinema Initiatives, LLC
*Digital Cinema System Specification*, Version 1.2
March 7, 2008

6. Gerhardt, Francis H., SMPTE Color Sensitometry Subcommittee Chairman
*Principles of Color Sensitometry*
SMPTE 1962

7. Hummel, Rob, Editor
American Cinematographer Manual, Ninth Edition
ASC Press 2004

8. IBM
*Cell Broadband Engine Programming Handbook*
May 2008

9. Kennel, Glenn
*Color and Mastering for Digital Cinema*
Focal Press 2007

10. Lallain, Cédric
"A 4x4 Matrix Inverse"
Cell BE web forum article 2008

11. Malacara, Daniel
Color Vision and Colorimetry: Theory and Applications
SPIE Press 2002

12. Patterson, Richard
*Evaluation Density Metrics for Scanning Motion Picture Negatives*
SMPTE Motion Imaging Journal
May/June 2008

13. Poynton, Charles
*Digital Video and HDTV Algorithms and Interfaces*
Morgan Kaufmann Publishers 2003

14. Probst, Christopher
"Color Conundrum"
*American Cinematographer*, May 1997
ASC Press

15. Snider, David; Kennel, Glenn; Ken Curry; and Michael McCrackan
"Digital Motion-Picture Exchange: File Format and Calibration"
SMPTE Journal, August 1993

16. Sony Corporation Whitepaper
*The Basics of Cell Computing Technology*

17. Swartz, Charles S.
*Understanding Digital Cinema*
Focal Press 2006

18. SMPTE Standard 268M-1994
"File Format for Digital Moving Picture Exchange (DPX)"
SMPTE Journal, August 1993

19. Wyszacki, Günther and Stiles, W.S.
*Color Science: Concepts and Methods, Quantitative Data and Formulae*, Second Edition
John Wiley & Sons, INC Wiley Classic Library Edition 2000